

Changes in the surface morphology of polycarbonate induced by fretting

P. A. HIGHAM*, B. BETHUNE, F. H. STOTT

Corrosion and Protection Centre, University of Manchester Institute of Science and Technology, Manchester, UK

Although fretting damage is normally associated with contacting metal surfaces subjected to relative oscillatory slip of a few microns amplitude, it can also occur when polymers are in contact with metals. The fretting damage between polycarbonate–steel surfaces is made up of iron oxide debris from the steel surface and the formation of cracks on, and fibres from, the polymer surface. Cracking and flow is the result of hysteretic heating arising from the low thermal conductivity and relatively high damping capacity of the polymer. Since the rate of heating is dependent on the energy imparted to the process, increasing the amplitude of slip reduces the time to cracking and polymer flow. Neither cracking nor flow is influenced by gaseous environments and sites producing fibres remain active until the encroachment of iron oxide from adjacent slip regions gradually stifles fibre formation.

1. Introduction

Fretting can be considered a form of wear which occurs between contacting surfaces subjected to small oscillatory relative displacement (amplitude $< 120 \mu\text{m}$). In any situation where surfaces are in contact and are subject to vibration there is the possibility of relative motion between them and thus of fretting taking place. It is obvious, therefore, that the probability of encountering fretting in machines and engineering structures is extremely high. With the increased use of polymers as engineering materials, there are numerous applications where they are expected to function in close contact with metal surfaces; for instance in bearings and as 'anti-fretting' layers.

The most common form of fretting occurs between steel surfaces where the generation of oxide debris, pits and cracks is termed fretting corrosion [1]. However the occurrence of fretting damage between steel–polymer surfaces where metallic debris is produced has also been reported in most commercially available polymers [2–5] and one reference [2] has been made to the promotion of fretting corrosion by PTFE, though whether this was due to non-polymer components which are

normally incorporated in commercial PTFE bearings is not made clear.

Because of the growing interest in the behaviour of polymer–metal couples, particularly in bearing conditions, extensive investigation of metal–polymer surfaces in the fretting situation has been made and the results discussed here are part of this work. In this paper, we are concerned with the damage to the polymer surface, which involves the formation of fibres and surface cracks after fretting against mild steel. Elsewhere the effects of the various fretting parameters, such as load, amplitude, frequency, number of cycles and environment, on the amount of metallic wear [6], the effects of polymer composition on the metallic wear [7] and the characteristics of the wear debris and the mechanisms of metallic wear [8] have been reported.

The wear of the steel surface consisted of the removal of the original air-formed film, rapid oxidation of the exposed metal to form $\alpha\text{-Fe}_2\text{O}_3$ and transfer of that oxide as very small single-crystal platelets, 35 to 50 nm diameter, to the polymer surface. The amount of wear and the particle size of the transferred oxide is very depen-

*Present address: Department of Aeronautical and Mechanical Engineering, University of Salford, Salford, UK.

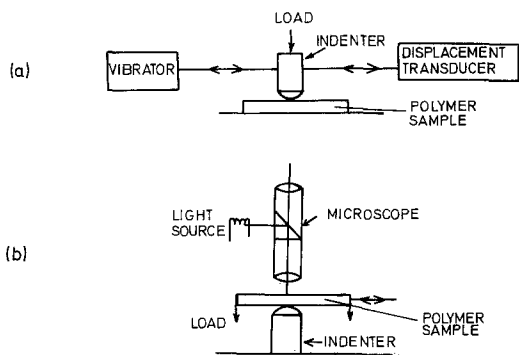


Figure 1 Schematic diagram of apparatus, (a) normal arrangement (b) for direct viewing.

dent on the adhesive properties of the contacting polymer. Environmentally, moisture plays a major role in the oxide particle formation and it is believed that the final formation of single crystals of $\alpha\text{-Fe}_2\text{O}_3$ platelets are evidence of a local rise in temperature associated with the fretting process.

2. Experimental details

The fretting apparatus has been described in detail elsewhere [6] and is shown schematically in Fig. 1a. Normally a spherically tipped, 4 mm radius, steel indenter is directly loaded against a polymer flat. The indenter is then subjected to a reciprocating tangential force which produces slip in the outer annular contact region. In some experiments the steel indenter is clamped to the base of the apparatus and the flat polymer samples loaded against it and subjected to a reciprocating tangential force, Fig. 1b. In the case of transparent polymers this arrangement allowed the fretting process to be viewed continuously with an optical microscope.

The experimental parameters and specimen composition are listed in Table I. The tip of the steel indenter was profile ground on a 120 grit

TABLE I

Operating parameters	Frequency 10 to 150 Hz, Amplitude 2 to 30 μm , load 130 to 830 g.
Environments	Laboratory Atmosphere (50 \pm % r.h.) Dry oxygen (< 0.3% N_2 , < 6 vpm H_2O) Dry nitrogen (< 10 vpm O_2 , < 15 vpm H_2O) Dry argon (< 4 vpm O_2 , 2 vpm H_2O)
Steel composition	C 0.18%, Mn 0.73%, Si 0.23%, Ni 0.17%, Cr 0.13%
Polymer	Polycarbonate (Makrolon)

abrasive wheel and polished using, successively, 60, 45, 25 and 14 μm diamond lapping compounds. After annealing at 900°C for 1 h in a vacuum of 10^{-2} Pa, the tip was polished using 6 and 3 μm diamond compounds before being thoroughly degreased ready for immediate use. The polycarbonate samples (20 mm \times 20 mm) were cut from 3 mm sheet, and were used in the as-received condition after removal of the protective surface paper. Most experiments were carried out in laboratory air but, in some cases, fretting was performed in an environmental chamber which was purged with dried atmospheres of oxygen, nitrogen and argon. After fretting, the surfaces were examined using optical and scanning electron microscopes.

3. Fretting-induced morphological changes

3.1. Surface cracking in the slip region

The appearance of surface cracks was the first feature to be observed on the fretted polymer surface. A number of small cracks were initiated at the inner edge of the slip annulus, at the slip-no-slip boundary at the extremes of the slip direction, Fig. 2a. As fretting proceeded, crack growth led to their coalescence to form two curved cracks, symmetrical with the area of contact but having larger diameters, Fig. 2b. The slip annulus was the region to which iron oxide debris was transferred from the metal to the polymer surface and the cracks form a sharp inner boundary for the accumulating oxide particles, Fig. 3.

Cracks were not observed immediately at the start of fretting and the critical number of cycles to crack initiation depended on the amplitude of slip, Fig. 4. No cracking occurred when the amplitude was below 3.0 μm , within the range of applied load 130 g to 530 g, and although a decrease in the amplitude of slip delayed the onset of cracking, a change in the applied load did not affect it. The onset of cracking was not found to depend on the frequency of vibration within the range tested (120 to 10 Hz).

Variations in the gaseous environment surrounding the fretting specimens had no effect on crack formation.

3.2. Polymer flow in the no-slip region

After the formation of the curved surface cracks it became obvious that polymer material in the central no-slip area of the wear scar was moving outwards on both sides normal to the directions of

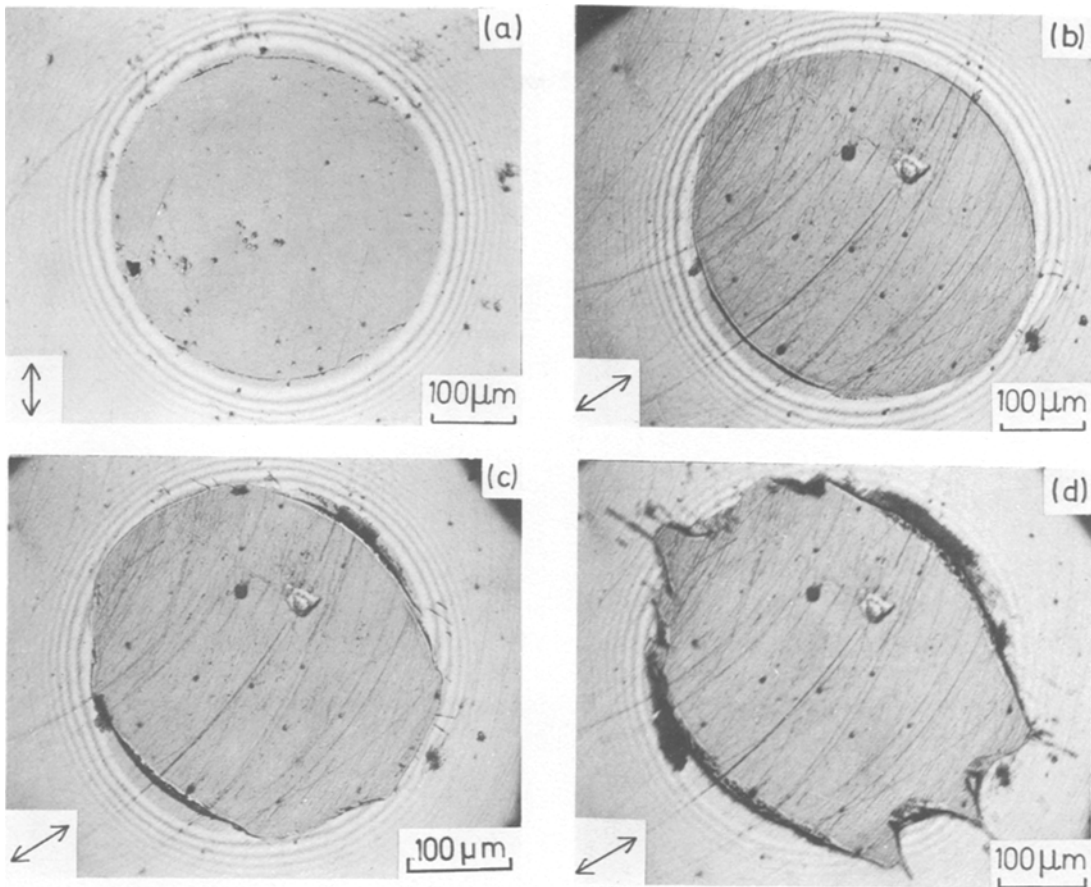


Figure 2 Optical micrograph of contact area (direct view). Fretting carried out under a load of 330 g and at a frequency of 60 Hz. (a) $6.9 \mu\text{m}$, 5.5×10^4 cycles. (b) $11.5 \mu\text{m}$, 4×10^4 cycles. (c) $11.5 \mu\text{m}$, 8×10^4 cycles (d) $11.5 \mu\text{m}$, 1.6×10^5 cycles.

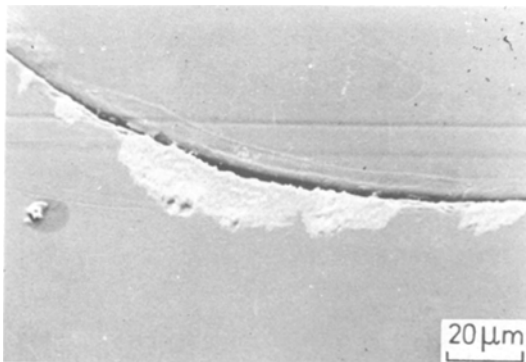


Figure 3 Scanning electron micrograph showing crack formed at the slip–no-slip boundary. Iron oxide debris, light area, is accumulating on the slip side of the crack.

slip, Fig. 2c. Initially a regular expansion sideways was maintained but gradually the leading edge took on a serrated appearance, Fig. 2d. The number of serrations formed depended on the

amplitude of slip, the higher the amplitude the fewer the serrations formed.

The outward movement of the polymer material was accompanied by the formation of tears and fissures on the surface of the polymer sample. These features first occurred in the central no-slip region in a line adjacent to the primary cracks, Fig. 5. Later with the formation of the serrations, further voids appeared along the edges of the outward flowing polymer, Fig. 6.

3.3. Polymer fibre formation

When the serrated areas became fully developed and ceased to grow outwards, fibres began to form at their tips, Fig. 7a. Direct observation of fibre formation revealed that the serrated tips were very active, each tip producing a number of fibres which quickly grew outwards from the contact region, if a fibre became detached, it was immediately replaced by the growth of a fresh fibre.

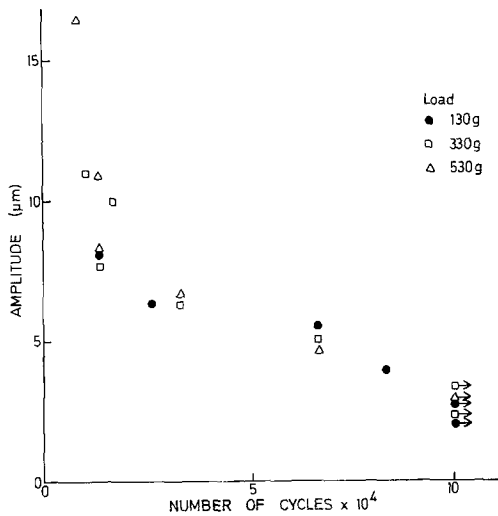


Figure 4 Number of cycles to cracking plotted against amplitude of slip at a frequency of 60 Hz.

At the peak of fibre production, the area surrounding the contact region was animated with a twisting mass of fibres which grew outwards to a length of a few millimeters, Fig. 7b.

The amplitude of slip plays a large part in influencing the formation of the fibres. No fibres were

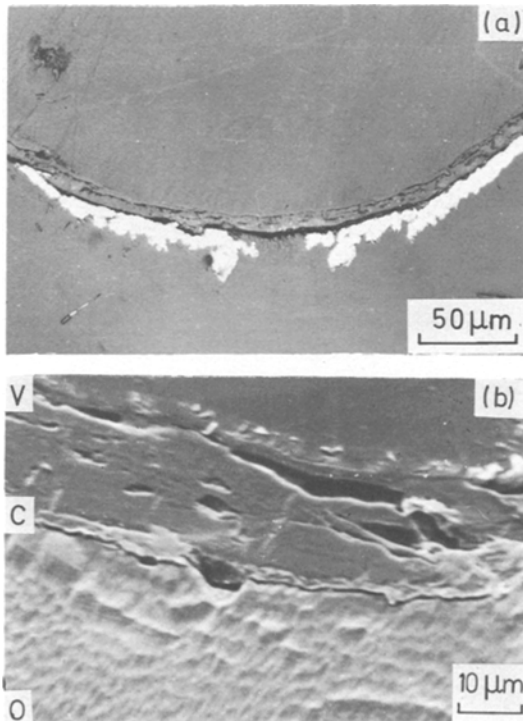


Figure 5 Voids and tears formed inside slip–no-slip crack boundary. (a) optical micrograph (while region is iron oxide debris), (b) scanning electron micrograph (oxide O, crack C, voids V).

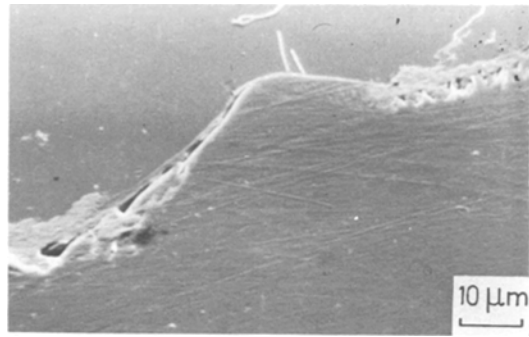


Figure 6 Scanning electron micrograph showing voids formed along the edge of a serration.

observed when the amplitude is low, 2.8 µm. At an amplitude of 3.5 µm, Fig. 8, a few short fibres are formed and these increase in number, length and diameter with increasing amplitude. Finally, at high amplitudes, 16.5 µm bulk extrusion of the polymer from the tip of the serrations occurred and fibre formation ceased, Fig. 9.

Fig. 10 presents a series of results indicating how fibre formations varied with the experimental conditions. From these results it can be seen that

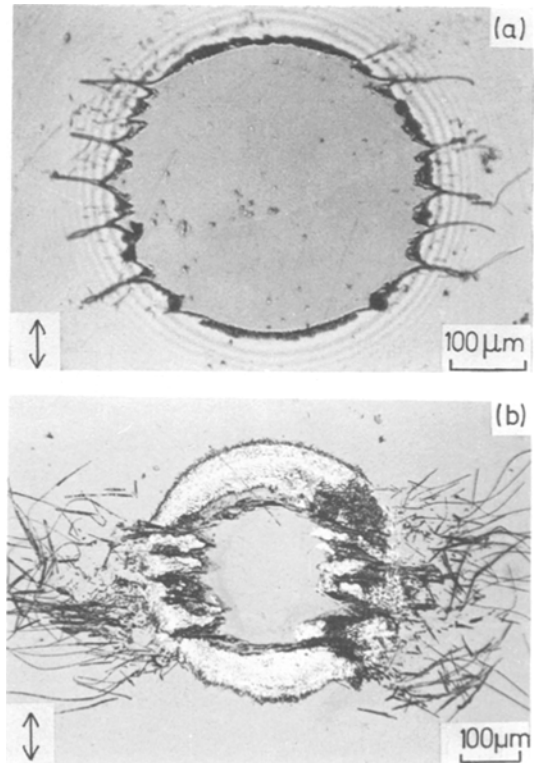


Figure 7 Optical micrograph of contact area showing fibre formation (a) Direct view (6.9 µm, 330 g, 60 Hz, 8×10^5 cycles), (b) Normal view (11 µm, 330 g, 60 Hz, 1.2×10^6 cycles).

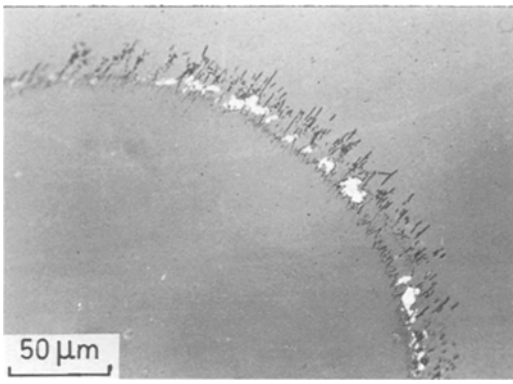


Figure 8 Optical micrograph. Normal view (3.5 μm, 330 g, 60 Hz, 5×10^5 cycles). Showing the small fibres and serrations formed at low amplitudes of slip.

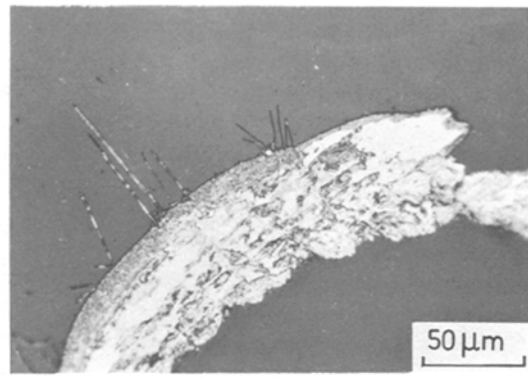


Figure 11 Optical micrograph (normal view). Fibre formation stifled by iron oxide, (light area).

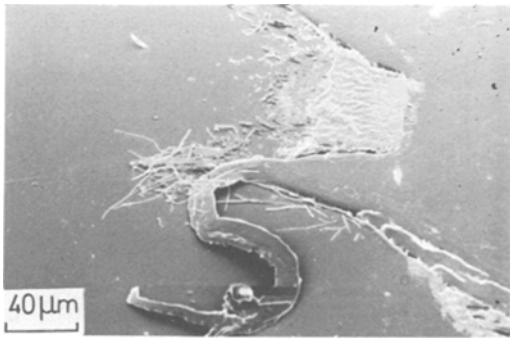


Figure 9 Scanning electron micrograph. (16.5 μm, 530 g, 60 Hz, 4×10^5 cycles). Showing the bulk polymer extrusion from the serration tip at high amplitudes of slip. Iron oxide debris, light area, is accumulating between the serrations.

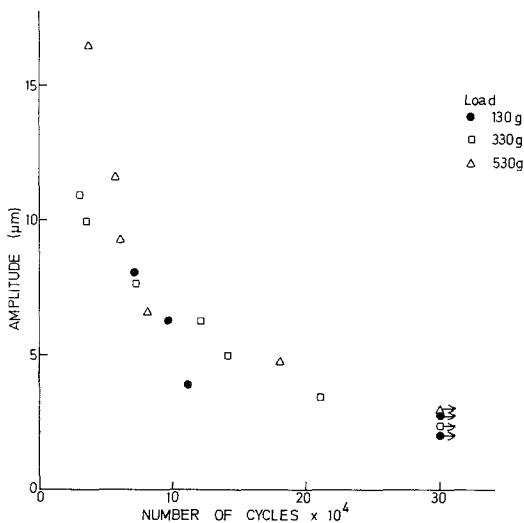


Figure 10 Number of cycles to formation of fibres plotted against amplitude of slip at a frequency of 60 Hz.

irrespective of the normal load, an increase in the amplitude of slip results in a decrease in the time to the first appearance of fibres.

Fibre growth did not always proceed unhindered and the incorporation of metallic oxide debris could lead to the stifling of the active serrations as the debris chokes up the polymer movement. Although the iron oxide first appeared in the slip region outside the curved surface cracks, Figs. 3 and 5, it later appeared in the areas between the serrations, Fig. 9. The amount of debris increased with the number of cycles and gradually encroached into the serrated areas. Finally when the serrations became covered in oxide debris, Fig. 11, fibre formation ceased. Increasing the amplitude of slip increases the period before fibre formation was stopped, and if the amplitude was large enough, $> 10 \mu\text{m}$, fibres were produced indefinitely. When the oxide debris began to spread into the serrations it became entrapped in the flowing polymer and finally appeared in the fibres, Fig. 12. Direct observation of fibre formation from the serrations reveals that they are growing with a spinning motion that leads to the fibres having a twisted form, Fig. 12a. The inclusion of the hard oxide powder in the spinning fibre led to the abrasion of the polymer surface and the formation of channels in the region of fibre formation, Fig. 13. As more oxide entered the flowing polymer the spiralling of the spinning fibre became more pronounced and finally the fibres broke down into small spheres, Fig. 14.

If the production of iron oxide debris was not sufficient to stop fibre formation, then there was a gradual decrease in the number of fibres produced as the loss of polymer from the central region led

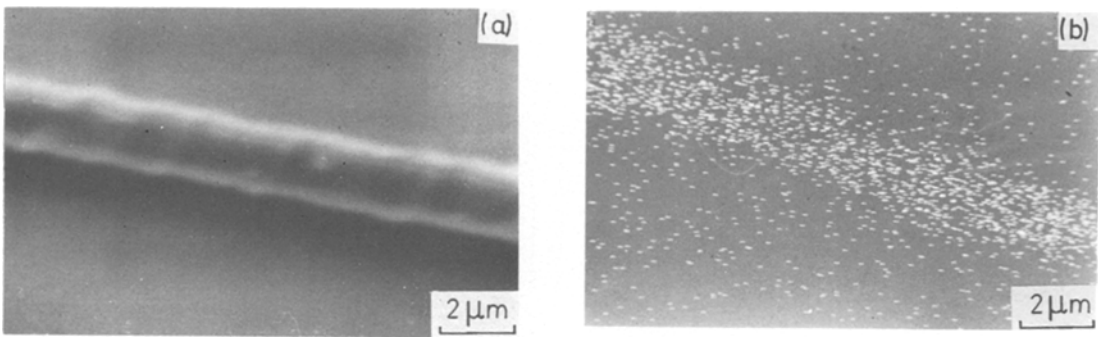


Figure 12 (a) Scanning electron micrographs of a fibre (b) Elemental distribution of iron in (a).

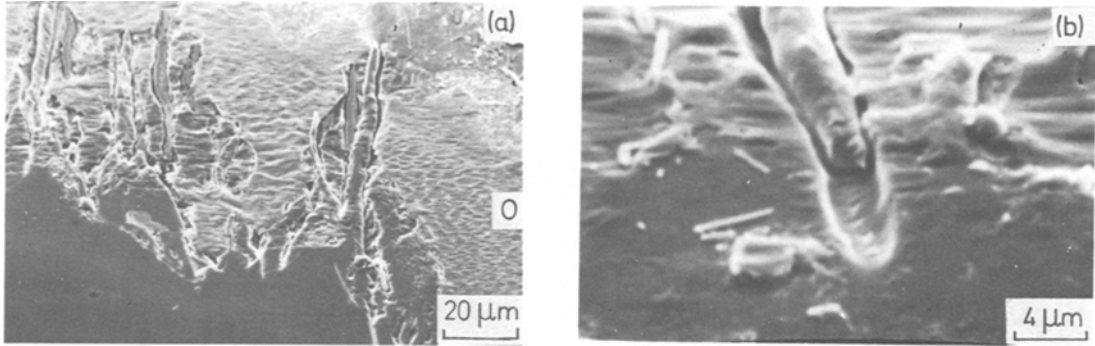


Figure 13 Scanning electron micrographs showing fibres channeling through the polymer matrix (area covered by iron oxide O).

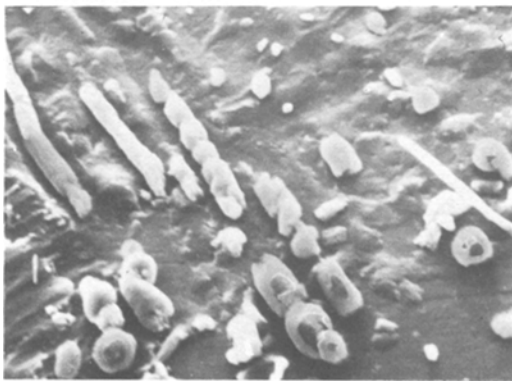


Figure 14 Scanning electron micrograph showing the breakdown of fibres due to their high iron oxide debris content.

to a larger area of contact. Profile measurements across the contact area on the flat polymer surface after removal of the indenter indicated that the loss of polymer had led to the formation of a deep groove surrounding a greatly reduced central no-slip area, Fig. 15.

The surrounding gaseous environment was found to have no effect on the fibre formation. However, since the dry atmospheres of argon, nitrogen or oxygen, prevented the formation of

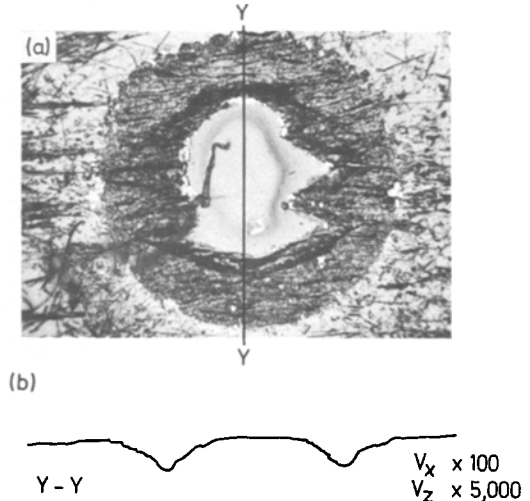


Figure 15 (a) Optical micrograph showing the fretting damage after prolonged cycling ($11.5 \mu\text{m}$, 330 g , 60 Hz , 6×10^6 cycles). (b) Profile trace corresponding to Y-Y in (a).

oxide debris [8], fibre formation under these conditions continued unchecked.

4. Discussion

Although relatively soft polymeric materials can cause little serious wear of steel under uni-

directional sliding, when the slip becomes oscillatory and confined to small amplitudes, metal wear may be produced by a wide range of polymers. The seriousness of this in causing loss of fit on a bearing shaft or the production of oxide debris in a clean environment is obvious. In this work, the fretting damage produced on the polymer surface has been examined. The cracking and the flow of polymer to form fibres is potentially just as serious as the fretting wear of the steel. Practically, the flow of polymer could lead to loss of fit and possibly seizure under bearing conditions, the production of fibres could cause contaminants where clean conditions are desirable, and the surface cracks could act as nuclei for environmental stress cracking.

In these experiments, the chosen contact geometry of a sphere on a flat was made because it provides a simple symmetrical stress system which is well understood and allows the changes in surface morphology to be related easily to specific slip-no-slip conditions.

Micro-fracture at the periphery of contact is produced on the surface of brittle materials when indented by a hard sphere. Where indentation is accompanied by tangential stress, the critical load to produce cracking is reduced and a series of curved cracks are formed in the wake of a sliding indenter. Only polystyrene has been found to crack when indented by a hard steel sphere in air, other glassy amorphous polymers which are less brittle require the presence of a stress cracking environment to produce cracks in them [9].

The curved cracks formed under fretting conditions appear very similar to those formed under a sliding indenter. However as there is always a definite nucleation period before cracks are observed it is likely that their formation depends on a fatigue process due to cyclic stressing.

The fatigue failure of materials subjected to cyclic loading occurs at stresses below those normally sustained under static loading and, although normally associated with metal failure, fatigue is observed in thermoplastics. Polymers, being viscoelastic, are relatively high-damping materials and the cyclic energy applied to them is dissipated by internal damping as heat. Experiments on unnotched polymer fatigue samples where the temperature was monitored continuously [10], have shown that at constant load the cycling frequency determined the hysteretic heating. Although the temperature rise per cycle may be low, e.g. 0.01°C ,

because of the poor thermal conductivity of polymers, a significant temperature rise can be obtained with continued cycling and eventually the glass transition temperature may be reached. Two forms of failure are observed [11], the specimen is either fractured, or else it is softened to the extent that it can no longer stand the applied stress. Fracture occurs when high thermal gradients set up excessive thermal stresses and failure occurs along lines of the maximum shear stress [12]. Softening occurs when the temperature exceeds that of the glass transition and the modulus is then significantly lowered.

Under fretting conditions, both types of failure have been seen in the area of contact. First, after an incubation period, as heat is generated and the temperature builds up, cracking occurs along the boundary of the slip-no-slip region where the shear stress and temperature are a maximum. When the central region reaches the glass transition temperature, (T_g polycarbonate = 145°C), the softened polymer is forced outwards by the compressive stresses beneath the steel indenter. Under the influence of the shear stresses at the contact periphery, flow takes place from both sides of the contact area normal to the slip direction. This preferred direction of flow leads to the shaping of the polymer front into serrations as surface tension maintains the minimum distance between the solid surfaces. At low amplitudes, only a little flow occurs over a large front and a lot of small serrations occur, while, at high amplitudes, bulk flow leads to only a few large serrations. Likewise fibres that are spun out of the tips of serrations grow in size and length with increasing amplitude. At the highest amplitudes investigated, the outward flow was so great that fibres ceased to be spun and a flat ribbon of polymer was extruded from the tip of the serration. The movement of polymer outwards leads to the formation of tears and voids, particularly where the flowing polymer occurs adjacent to the cooler, more rigid material along the edges of contact. In the final stages of fretting, the gross outflow of polymer is seen to have left a large groove round the contact area, Fig. 15.

As the heat generation which leads to fracture and polymer softening depends on how fast the external work is applied, the amplitude of slip is a controlling factor. The higher the amplitude, the more rapid the heating and the shorter the period before cracking and flow occurs. It might be ex-

pected that increasing the frequency would have a similar effect but this was not found to be the case within the range 120 to 10 Hz examined.

Although the results presented here have dealt solely with polycarbonate, similar morphological changes have been observed with other polymers [13]. Cracking is confined to the amorphous glassy polymers and is encountered in polystyrene, polyvinyl chloride and polysulphone. Fibre formation is observed in both amorphous and crystalline polymers and is found in polystyrene, polyvinyl chloride, polysulphone, nylon, and polyethylene. The damping capacity of polymers is greatest in the amorphous state and increasing crystallinity leads to an improved fatigue life, an improvement that is aided by a slight increase in modulus which accompanies crystallinity [10]. This structural factor also influences the changes in the polymer surface during fretting and it was found that only the amorphous polymers cracked. Both amorphous and crystalline polymers were sufficiently softened by hysteretic heating to allow the outward flow of polymers and fibre formation.

In the region of flowing polymer no slip occurs between the polymer and steel surface so no metal oxide is formed. Oxide debris accumulating in the slip regions adjacent to the serrations is finally incorporated into the flowing polymer and consequently the fibres. The inclusion of oxide into the spinning fibres allows them to abrade channels in the polymer matrix. As the oxide content increases the mixture becomes less fluid and the fibres are seen to break down into ball like structures. Finally, the oxide content becomes so great that the flow and fibre formation ceases.

Fatigue tests involving unnotched specimens of thermoplastics have, unlike metals, been found to be insensitive to the surrounding gaseous environ-

ments [14]. This was also observed under fretting conditions when no change was observed in cracking and flow of the polymer for a range of gaseous environments.

Acknowledgements

The authors thank Professor G. C. Wood for the provision of facilities. One of them (PAH) thanks the Science Research Council for the provision of a Research Studentship during the period in which this work was carried out. Bayer Plastics Limited kindly provided the polycarbonate.

References

1. R. B. WATERHOUSE, "Fretting Corrosion", (Pergamon Press, London, 1972).
2. A. CHAMBAUD, *Revue du Nickel* **20** (1954) 30.
3. K. H. R. WRIGHT, *Proc. Inst. Mech. Eng.* **1B** (1952-53) 556.
4. W. P. MASON and S. D. WHILE, *Bell Syst. Tech. J.* **31** (1952) 469.
5. N. OHAMAE, K. KOBAYASHI and T. TSUKIGOE, *Wear* **29** (1974) 345.
6. P. A. HIGHAM, F. H. STOTT and B. BETHUNE, *Wear*, to be published.
7. *Idem, ibid*, to be published.
8. *Idem, Corros. Sci.*, to be published.
9. B. BETHUNE, *J. Mater. Sci.* **11** (1976) 199.
10. M. N. RIDDELL, G. P. KOO and J. L. O'TOOLE, *Polymer Eng. Sci.* **6** (1966) 363.
11. D. A. OPP, D. W. SKINNER and R. J. WIKTOREK, *ibid* **9** (1969) 121.
12. T. R. TAUCHERT and S. M. AFZAL, *J. Appl. Phys.* **38** (1967) 4568.
13. P. A. HIGHAM, Ph.D. Thesis, University of Manchester, 1976.
14. R. W. HERTZBERG, J. A. MANSON and M. SKIBO, *Polymer Eng. Sci.* **15** (1975) 252.

Received 15 March and accepted 13 May 1977.